

Glacial-interglacial seawater isotope change near the Chilean Margin as reflected by $\delta^2\text{H}$ values of C₃₇ alkenones.

Katrin Hättig¹, Devika Varma¹, Stefan Schouten^{1,2}, Marcel T. J. van der Meer¹

¹ Department of Marine Microbiology and Biogeochemistry, NIOZ Royal Netherlands Institute for Sea Research, Texel, the Netherlands

² Department of Earth Sciences, Faculty of Geosciences, Utrecht University, Utrecht, the Netherlands

Correspondence to: Katrin Hättig (katrin.haettig@nioz.nl)

Abstract. Stable hydrogen isotopic compositions of long-chain alkenones with 37 carbon atoms ($\delta^2\text{H}_{\text{C}37}$) have been shown to reflect seawater salinity in culture and environmental studies and this potential sea surface salinity proxy has been applied to several down core records from different regions. However, previous studies were based solely on a single sediment core and often suggested unlikely large changes in salinity based on existing proxy calibrations. Here we present a new $\delta^2\text{H}_{\text{C}37}$ record, in combination with oxygen isotopes of benthic foraminifera from the same samples, from a sediment core from the Chilean Margin (ODP site 1235). The observed negative shift in $\delta^2\text{H}_{\text{C}37}$ of 20‰ during the last deglaciation was identical to that of a previously published $\delta^2\text{H}_{\text{C}37}$ record from the nearby located, but deeper, ODP core 1234, suggesting a regionally consistent shift in $\delta^2\text{H}_{\text{C}37}$. This change translates into a negative hydrogen isotope shift of the surface seawater of ca. 14‰, similar to glacial-interglacial reconstructions based on other $\delta^2\text{H}_{\text{C}37}$ records. The reconstructed bottom seawater oxygen isotope change based on benthic foraminifera during the last deglaciation is approximately -0.8‰, in line with previous studies. When translated into hydrogen isotopes of bottom seawater using the modern open-ocean water line, this would suggest a negative change of ca. 5‰, smaller than the reconstructed surface seawater shift based on alkenones. The larger change in surface water isotopes suggests that it experienced more freshening during the Holocene than bottom waters, either due to increased freshwater input or reduced evaporation, or a combination of the two.

1 Introduction

The stable oxygen and hydrogen isotope composition of seawater ($\delta^{18}\text{O}_{\text{sw}}$ and $\delta^2\text{H}_{\text{sw}}$, respectively) reveal crucial information about (sea)water physicochemical properties, which improves our understanding of past global ocean current dynamics and changes therein. Several oceanographic factors can cause shifts in the isotopic composition of seawater: for example, the bottom seawater isotopic composition depends on the source area of the water and reflects the history of advection associated with transport, mixing, upwelling and downwelling of ocean currents (Rohling and Cooke, 1999). Regional factors affecting the surface seawater isotopic composition are the evaporation-precipitation balance, river water input, iceberg melting, and the local climate regime (Rohling and Cooke, 1999). On a more global level, land ice formation is an important process that affects oxygen and hydrogen isotopes of seawater, where during glacial periods large amounts of water with relatively low, more

negative, $\delta^{18}\text{O}$ and $\delta^2\text{H}$ values are stored as ice on land, increasing seawater $\delta^{18}\text{O}$ values (e.g. Schrag et al., 2002). Decreasing global ice volume during warmer interglacials, releases this fresh, low-density water with relatively low $\delta^{18}\text{O}$ and $\delta^2\text{H}$ values into the surface ocean (Rohling and Bigg, 1998). Since both seawater isotopes and salinity increase as a result of evaporation and decrease as a result of precipitation or freshwater input, seawater isotopes and salinity are tightly coupled (Rohling 2007; 35 Craig 1961; Craig and Gordon 1965). Therefore, seawater isotopes are often reconstructed and used to infer past salinity changes (e.g. Lamy et al., 2002; Schrag et al., 2002; Rousselle et al., 2013).

There are several methods available to reconstruct the isotopic composition of seawater. The stable oxygen isotopic composition of foraminifera ($\delta^{18}\text{O}_{\text{foram}}$) is a function of $\delta^{18}\text{O}_{\text{sw}}$ and calcification temperature (Bemis et al., 1998; Epstein et al., 1953; Shackleton, 1974) with a minor effect of carbonate ion concentration (Spero et al., 1997). Temperature corrected 40 $\delta^{18}\text{O}_{\text{foram}}$ is thus assumed to reflect $\delta^{18}\text{O}_{\text{sw}}$, though with some uncertainty (Duplessy et al., 1991; Rostek et al., 1993). Generally, temperature corrections of $\delta^{18}\text{O}_{\text{foram}}$ to reconstruct $\delta^{18}\text{O}_{\text{sw}}$ are done based on temperature proxies derived from the same foraminifera, such as Mg/Ca (e.g. Billups et al., 2002, 2003; Lear et al., 2000, 2004, 2015; Martin et al., 2002) or carbonate clumped isotopes (Δ_{47}) (e.g. Petersen et al., 2015). In some cases, independent temperature proxies based on organic geochemical indices, such as U^{237} and TEX_{86} (Brassell et al., 1986; Prahl et al., 1987; Schouten et al., 2003), are used to 45 correct for temperature (Rostek et al., 1993, 1997). Several studies based on $\delta^{18}\text{O}_{\text{foram}}$ -records, $\delta^{18}\text{O}$ values of porewaters and modelling, estimate a negative global average change of 0.8–1.1‰ in the oxygen isotope ratio of seawater during the last deglaciation (e.g. Adkins and Schrag et al., 2001; Adkins et al., 2002; Duplessy et al., 2002; Oba et al., 2004; Waelbroeck et al., 2002). Based on this, the salinity change is thought to be around 1–2 psu (Adkins et al., 2002; Broecker, 2002). Deriving 50 salinity from local $\delta^{18}\text{O}_{\text{sw}}$ estimates, i.e. those corrected for global $\delta^{18}\text{O}_{\text{sw}}$ changes requires knowledge of the regional relationship between $\delta^{18}\text{O}_{\text{sw}}$ and salinity (LeGrande and Schmidt, 2006; Rohling, 2007). However, it is uncertain whether this relationship is consistent through time.

The hydrogen isotopic composition of seawater is more difficult to reconstruct. Schrag et al. (2002) measured the hydrogen isotopic compositions of pore fluids in deep-sea sediments and showed a negative shift of 6–9‰ in the hydrogen isotopic composition of bottom seawater ($\delta^2\text{H}_{\text{BSW}}$) during the last glacial to interglacial transition. A potential proxy for reconstructing 55 surface seawater ($\delta^2\text{H}_{\text{SSW}}$) is based on the combined hydrogen isotopic composition of long-chain alkenones with 37 carbon atoms and two and three double bonds $\delta^2\text{H}_{\text{C37}}$ derived from haptophyte algae. Culture studies show that the hydrogen isotopic fractionation of phototrophic organisms depends not only on the hydrogen isotopic composition of seawater but also on salinity (M'Boule et al., 2014; Sachs et al., 2016; Schouten et al., 2006; Weiss et al., 2017a; Zhang et al., 2009; Zhang et al., 2007). However, the response of $\delta^2\text{H}_{\text{C37}}$ to salinity varies significantly between haptophyte species (M'Boule et al., 2014; Sachs et al., 60 2016; Schouten et al., 2006), as well as in different environmental settings where sometimes no impact of salinity on $\delta^2\text{H}_{\text{C37}}$ is found (Gould et al., 2019; Häggi et al., 2015; Mitsunaga et al., 2022; Weiss et al., 2019b). These differences or absences in response of $\delta^2\text{H}$ to salinity make quantitatively constraining past salinity changes difficult. Downcore records show a decrease of 16–25‰ in $\delta^2\text{H}_{\text{C37}}$ (when corrected for ice volume 9–18‰) for the last deglaciation to Recent depending on the site (Kasper et al., 2014; Pahnke et al., 2007; Petrick et al., 2015; Simon et al., 2015; Weiss et al., 2019a). Based on these results, Weiss et

65 a1. (2019b) reconstructed glacial–interglacial salinity changes of 5–19 psu, based on multiple different $\delta^2\text{H}_{\text{C}37}$ –salinity calibrations. These reconstructed glacial–interglacial salinity changes are much larger than based on $\delta^{18}\text{O}$ and ice volume modelling (e.g. Oba et al., 2004; Adkins et al., 2002). Therefore, Weiss et al. (2019b) concluded that either glacial–interglacial salinity changes are larger than previously assumed or the paleo sensitivity of $\delta^2\text{H}_{\text{C}37}$ to salinity changes was higher in the past than observed in modern–day environments and cultures.

70 A different approach is to correlate $\delta^2\text{H}_{\text{C}37}$ with $\delta^2\text{H}_{\text{SSW}}$ rather than salinity. Gould et al. (2019) observed a statistically significant $\delta^2\text{H}_{\text{C}37}$ – $\delta^2\text{H}_{\text{SSW}}$ relationship with open–ocean suspended particulate organic matter (SPOM), and Mitsunaga et al. (2022) showed a statistically identical relationship based on core top sediments. This suggests that in the natural environment, the effects of factors like salinity, species composition (e.g. Chivall et al., 2014; M’Boule et al., 2014), light and nutrients (Sachs et al., 2015; van der Meer et al., 2015) on stable hydrogen isotope fractionation during biosynthesis may be less 75 important than the isotopic composition of seawater. This observation allows direct inference of $\delta^2\text{H}_{\text{SSW}}$ from $\delta^2\text{H}_{\text{C}37}$ without any additional correction, though this approach has not been applied yet to reconstruct past $\delta^2\text{H}_{\text{SSW}}$. Mitsunaga et al. (2022) did suggest a “global” LGM–Modern change of -12.7‰ in the hydrogen isotopic composition of alkenones based on the global $\delta^{18}\text{O}_{\text{sw}}$ shift, a waterline slope of 8 and their core top calibration. Similar as for $\delta^{18}\text{O}_{\text{sw}}$, reconstructed $\delta^2\text{H}_{\text{SSW}}$ can then be converted into salinity using modern–day correlations between surface $\delta^2\text{H}_{\text{SSW}}$ and salinity (LeGrande and Schmidt, 2006; 80 Rohling, 2007).

Here, we generated a $\delta^2\text{H}_{\text{C}37}$ and benthic $\delta^{18}\text{O}_{\text{foram}}$ record of ODP core 1235 from the Chilean Margin (Fig. 1) and compared this with the previously published hydrogen isotope (Weiss et al., 2019b) and temperature records (de Bar et al., 2018) from nearby ODP core 1234. Both cores are only ~12 km away from each other, though at a different water depths (489 m versus 85 1015 m) and are expected to record the same surface seawater signal (Mix et al., 2003). In contrast to Weiss et al. (2019b), we reconstructed $\delta^2\text{H}$ values of surface seawater and compared this to bottom seawater oxygen isotope values ($\delta^{18}\text{O}_{\text{BSW}}$) inferred from measured benthic foraminifera $\delta^{18}\text{O}$ values and used both to constrain relative salinity change during the deglaciation.

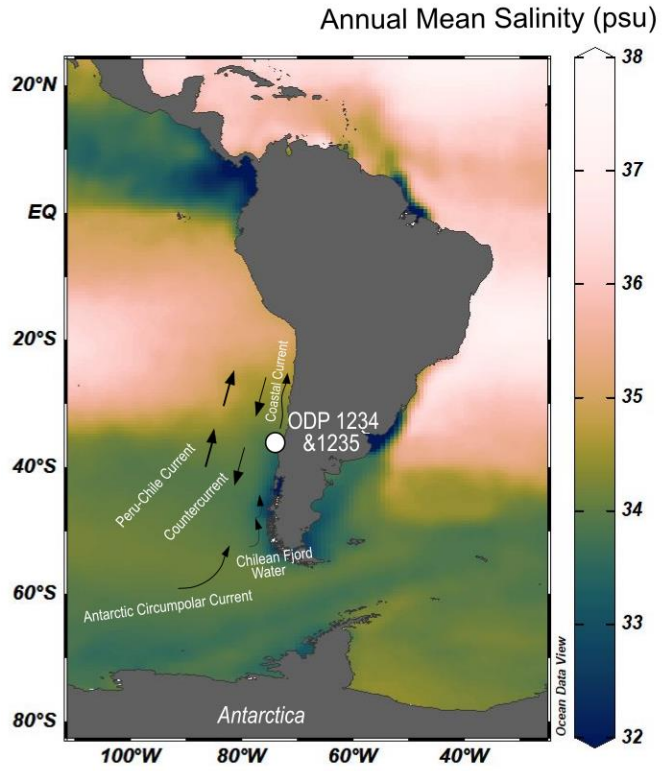


Figure 1: Map of sea surface salinity (data from Zweng et al., 2018, scientific colour map from Crameri et al., 2022) showing the sediment core locations of the neighbouring cores ODP 1234 and ODP 1235. The core location is influenced by three primary ocean currents: the Northward Peru–Chile Current and the Chilean Coastal Current, as well as the southward Peru–Chile Countercurrent. Those are fed by the Antarctic Circumpolar waters, and Chilean Fjord waters can also enter from the southeast the system.

2 Material and Methods

2.1 Geographic Setting

The ODP site 202-1235 was drilled at 36.16°S, 73.57°W at a relatively shallow water depth of 489 m (Fig. 1). The site is about 12 km away from the deeper neighbouring ODP 202–1234 site (36.22°S, 73.68°W, water depth 1015 m) in the southeast Pacific Ocean (Mix et al., 2003) (Fig. 1). These sites are located at the Chilean Margin which is influenced by surface and deep–water currents which cause upwelling, stimulating local productivity (Bakun, 1989). The setting is dynamic with southwesterly winds and freshwater runoff from the continent. The Antarctic Circumpolar Current (ACC) transports cold and saline water into the Peru–Chile Countercurrent which could be mixed with fresher fjord water, with a lower $\delta^2\text{H}$ value, along the southern margin (Lamy et al., 2002; Strub et al., 1998; De Bar et al., 2018). The present–day annual mean sea surface salinity in the study area is 33.8 ± 0.2 psu (World Ocean Atlas 2018, 0.25deg grid: Zweng et al., 2018).

2.2 Sampling and age model

Sediment samples of core ODP 1235 were split into two subsamples: Approximately 6 g of wet sediment was used for foraminiferal oxygen isotope analysis ($\delta^{18}\text{O}_{\text{foram}}$), and approximately 10 g of wet sediment was used for organic proxy analysis, 105 i.e. $U_{37}^{K'}$, TEX₈₆ (see Varma et al., 2023) and $\delta^2\text{H}_{\text{C}37}$ (this study). Samples were taken every 5–10 cm to cover a resolution of <2 ka, and a total of 27 samples were analysed for hydrogen isotopes.

The age–depth models for ODP 1235 and the neighbouring ODP core 1234 were both constructed with the statistical package Bacon (Blaauw and Christeny, 2011) using a Bayesian approach and are based on the radiocarbon ages of mixed benthic foraminifera (Muratli et al., 2010; this study, Table S1) as outlined by Varma et al. (2023). ODP 1234 has a mean sedimentation 110 rate of 20 cm ka⁻¹ and ODP 1235 a rate of 5 cm ka⁻¹.

2.3 Analysis of benthic foraminifera and long-chain alkenones

Stable oxygen isotopes were measured on the benthic foraminifera species *Uvigerina* with an automated carbonate device (Kiel IV, Thermo Scientific) connected to a Thermo Finnigan MAT 253 dual inlet isotope ratio mass spectrometer. The sample sizes were ca. 20 µg and contained 2–5 foraminifera shells (>150 µm). Replicate analyses of $\delta^{18}\text{O}$ values of the same sample 115 had a standard deviation of 0.016–0.2‰. NBS 19 limestone was used as the isotope calibration standard, and for drift detection and correction, a second standard, NFHS–1, was used. For both standards the standard deviation is within 0.1‰ for $\delta^{18}\text{O}$. All carbonate isotope data are given in ‰ relative to V–PDB (Vienna – Pee Dee Belemnite). Calculated $\delta^{18}\text{O}$ seawater values are given in ‰ relative to V–SMOW (Vienna – Standard Mean Ocean Water) with the accepted conversion value of 0.27‰ (Hut, 1987; Pearson, 2012).

120 The sediment split for organic analysis was extracted as described by Varma et al. (2023). Briefly, sediments were first freeze-dried and then extracted using an Dionex 350 Accelerated Solvent Extractor. The solvent from the total extract was first removed using a Turbovap and the last remaining water, if present, was removed using a small sodium sulfate column to obtain the total lipid extract (TLEs). The TLEs were separated into three fractions over a small aluminium oxide (Al_2O_3) column using hexane/ dichloromethane 9:1 (v:v) to elute first the apolar fraction, hexane/ DCM 1:1 (v:v) to elute the ketone (alkenone) 125 fraction, and dichloromethane/ methanol 1:1 (v:v) to elute the polar fraction. The ketone fractions were used for compound-specific hydrogen isotope ratio measurements of alkenones after being measured using a gas chromatograph coupled to a flame ionization detector (GC–FID) to determine the correct concentration and complexity of the fraction. Hydrogen isotope ratios were measured in duplicate using a gas chromatograph coupled to a Thermo Delta V isotope ratio mass spectrometer via high-temperature conversion reactor (Isolink I) and Conflo IV. The GC was equipped with an RTX–200 60 m column following 130 Weiss et al. (2019). We report the hydrogen isotope ratio, relative to V–SMOW, of the individual alkenones $\text{C}_{37:3}$ and $\text{C}_{37:2}$ and the integrated $\text{C}_{37} \delta^2\text{H}$ ratios determined by manual peak integration of the combined $\text{C}_{37:3}$ and $\text{C}_{37:2}$ peaks (van der Meer et al., 2013). The H_3+ factor was measured daily before running samples and shifted in time never more than 0.5 ppm/nA per day.

The performance and stability of the instrument were monitored by measuring a standard containing 15 *n*-alkanes at different concentrations (Mix B from A. Schimmelmann, Indiana University), at the start of each day. Samples were only run when the 135 average difference between the measured values for the Mix B standard and the certified values for this standard and their standard deviation were less than 5‰. With each sample, squalene and a C₃₀ *n*-alkane were coinjected to monitor system performance. Their measured values of -173 ±5‰ and -78 ±4‰ fit well with their predetermined values of -170 ±4‰ for squalene and -79 ±5‰ for the C₃₀ *n*-alkane.

2.4 Modern open-ocean isotopic composition of seawater

140 The relationship between δ¹⁸O–δ²H in the water–atmosphere environment can be described with the meteoric waterline (MWL) and is close to δ²H = 8 × δ¹⁸O + 10 according to Craig (1961) and Craig et al. (1965). To describe the relationship in surface ocean waters and investigate the potential for palaeoceanographic applications, Rohling (2007) correlated measured δ¹⁸O and δ²H of sampled ocean waters (top 250 m). We updated the dataset of Rohling (2007) with data from the Waterisotope Database 145 (2022) managed by Dr. G. Bowen (University of Utah) and published data from Gould et al. (2019), Weiss et al. (2019a) and Srivastava et al. (2010) (Fig. S2). This extended seawater isotope dataset contains 1550 datapoints from all water depths, not limited to the top 250 or 300 m, from the open-ocean:

$$\delta^2H_{SW} = 6.58 (\pm 0.07) \times \delta^{18}O_{SW} - 0.12 (\pm 0.03) \quad (R^2 = 0.82; \text{RMSE} = 3\text{‰}) \quad (1)$$

We will refer to this correlation as modern open-ocean water line (MOOWL). The relationship between the hydrogen isotopic composition of the surface seawater and the measured salinity in the modern open-ocean is based on the top 300 m water 150 depth, 424 datapoints are obtained from the extended seawater isotope dataset:

$$\delta^2H_{SW} = 3.53 (\pm 0.10) \times S - 122.57 (\pm 3.52) \quad (R^2 = 0.66; \text{RMSE} = 0.8 \text{ psu}) \quad (2)$$

Finally, the oxygen isotopic composition of the surface seawater (top 300 m) and the salinity were correlated based on 5602 datapoints:

$$\delta^{18}O_{SW} = 0.52 (\pm 0.01) \times S - 18.02 (\pm 0.18) \quad (R^2 = 0.64; \text{RMSE} = 0.8 \text{ psu}) \quad (3)$$

155 2.5 Calculation of Past Seawater Isotopes

2.5.1 Bottom Seawater

The oxygen isotopic composition of foraminifera depends mainly on the temperature of calcification (T) and isotope ratio of the water. McCrea (1950) published the first laboratory oxygen–isotope paleotemperature equation which was subsequently revised and extended to different calcite polymorphs and foraminifera species (e.g. Bemis et al., 1998; Cramer et al., 2011; 160 Epstein et al., 1953; Lynch-Stieglitz et al., 1999; Mulitza et al., 2003; O’Neil et al., 1969; Shackleton, 1974; Spero et al., 2003). The relationship can be described as the following, where d is the slope and c is the intercept:

$$T = c + d \times (\delta^{18}O_{foram} - \delta^{18}O_{SW}) \quad (4)$$

This relationship is used, in combination with temperature proxies, to reconstruct past $\delta^{18}O_{SW}$ values and, subsequently, obtain salinity estimations using the $\delta^{18}O_{SW}$ – salinity relationship (Lamy et al., 2002; Pearson, 2012; Tang and Stott, 1993; Ganssen et al., 2011). The most relevant paleotemperature equation for benthic foraminifera is currently from Lynch-Stieglitz et al. (1999), adjusted to V-SMOW by Cramer et al. (2011), where the $\delta^{18}O$ –paleotemperature relationship is estimated with the in field calibration of benthic foraminifera from the genera *Cibicidoides* and *Planulina* (Lynch-Stieglitz et al., 1999). *Uvigerina* genera $\delta^{18}O$ values are corrected to *Cibicidoides* and *Planulina* $\delta^{18}O$ values (e.g. Cramer et al., 2009, 2011). We adjusted the oxygen isotope ratios of *Uvigerina* in this study by 0.64‰ to fit with *Cibicidoides* and *Planulina* $\delta^{18}O$ values (i.e. Shackleton, 1974), these can be used, for the $\delta^{18}O_{BSW}$ reconstruction. Important to note is that $\delta^{18}O_{SW}$ is always measured on the V-SMOW scale, whereas calcite is standardized to V-PDB. The accepted value to convert V-PDB into V-SMOW at the time of Eq. (5) (Cramer et al., 2011) is 0.27‰.

$$T = 16.1 - 4.76 * (\delta^{18}O_{foram} - (\delta^{18}O_{BSW} - 0.27)) \quad (5)$$

Rearranged to $\delta^{18}O_{BSW}$:

$$175 \quad \delta^{18}O_{BSW} = \frac{-16.1 + 4.76 \times \delta^{18}O_{foram} + T}{4.76} + 0.27 \quad (6)$$

2.5.2. Surface Seawater

To estimate the δ^2H_{SSW} from the measured hydrogen isotopic composition of alkenones, we used the suspended organic matter calibration (SPOM) from Gould et al. (2019, reduced dataset):

$$\delta^2H_{C37} = 1.48 (\pm 0.4) \times \delta^2H_{SSW} - 199 (\pm 3) \quad (R^2 = 0.2; \text{RSME} = 5.8\%) \quad (7)$$

180 The environmental δ^2H_{C37} – δ^2H_{SSW} calibration from Gould et al. (2019) is based on alkenones from mainly open-ocean Group III haptophytes living in the Atlantic and Pacific ocean, covering large environmental differences such as salinity, temperature, nutrient concentrations and light intensity that in turn affect growth rate, for instance.

An alternative environmental calibration is the sediment core top study from Mitsunaga et al. (2022), where they extended and revised the data of Weiss et al. (2019a):

$$185 \quad \delta^2H_{C37} = 1.44 (\pm 0.13) \times \delta^2H_{SSW} - 191.62 (\pm 1.13) \quad (R^2 = 0.61; \text{RSME} = 7\%) \quad (8)$$

3 Results and Discussion

3.1 Reconstruction of bottom seawater isotopes based on foraminifera

The $\delta^{18}\text{O}$ values of benthic *Uvigerina* in ODP core 1235 range between 4.15‰ to 2.27‰ (Fig. 1). Between 40 to 27 ka, the $\delta^{18}\text{O}_{\text{foram}}$ is relatively stable with values between 3.13 to 3.96‰, followed by a decrease towards a value of 2.27‰ at 25 ka. Between 25 and 20 ka, the $\delta^{18}\text{O}_{\text{foram}}$ is higher with values of 3.7–4.15‰ and rapidly shifts by 1.6‰ to values of 2.27‰ in the uppermost sample. This record is consistent with ODP core 1234, showing a negative isotope shift from the LGM to 1 ka of ca. 1.7‰ in the $\delta^{18}\text{O}$ values of *Uvigerina* (de Bar et al., 2018).

To reconstruct $\delta^{18}\text{O}_{\text{BSW}}$, we need to reconstruct bottom water temperatures, which unfortunately, we were not able to do. To obtain some indications of temperature change, we used published SST records from the same core. The organic SST proxy $U_{37}^{K'}$ measured in this core (from Varma et al., 2023) indicates a temperature range of 11.9 °C to 16.9 °C, with relatively stable temperatures between 19 and 40 ka of ca. 13 °C and an increase of ca. 4 °C until 7 ka, after which it remained relatively stable (Fig. 1). The $\text{TEX}^{\text{H}}_{86}$ (from Varma et al., 2023) reveals temperatures between 10.3 and 15.9 °C and a similar increase of 4 °C from 20 ka till ca. 1 ka. Thus, both proxies indicate a LGM to recent temperature change of ca. 4 °C, consistent with SST proxy records from ODP core 1234 which also showed a temperature change of 4 °C from 20 ka till ca. 1 ka for both $\text{TEX}^{\text{H}}_{86}$ and $U_{37}^{K'}$ respectively (de Bar et al., 2018).

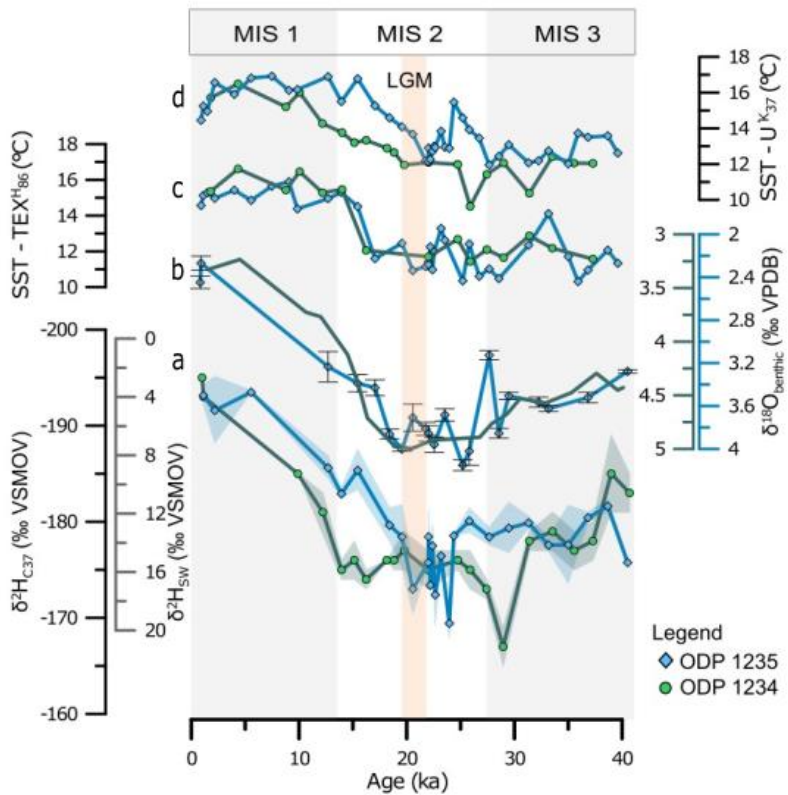
Adkins et al. (2002, 2001) suggested a similar bottom water temperature change of 4 °C for the Pacific, Southern, and Atlantic oceans, and thus we assume a similar temperature change for bottom water as reconstructed for surface water. Combined with the $\delta^{18}\text{O}$ values of *Uvigerina* this translates to a negative $\delta^{18}\text{O}_{\text{BSW}}$ shift of $0.8 \pm 0.2\text{‰}$ (averaged values with standard deviation of ODP 1235 and 1234 and a temperature error of $\pm 1\text{°C}$) from LGM to 1 ka using Eq. (6). This $\delta^{18}\text{O}_{\text{BSW}}$ shift subsequently translates, using the modern open-ocean $\delta^{18}\text{O}_{\text{sw}} - \delta^2\text{H}_{\text{sw}}$ relationship described in Eq. (1) and considering the error of the slope, to a $\delta^2\text{H}_{\text{BSW}}$ shift of $-5.5 \pm 1.8\text{‰}$ for bottom waters. This is similar to the values reported by Schrag et al. (2002), who measured oxygen and hydrogen isotopes of pore fluid from deep-sea sediments in the Southern and Northern Atlantic Ocean and observed a negative shift in $\Delta\delta^{18}\text{O}_{\text{BSW}}$ of 0.7–1.1‰ and $\Delta\delta^2\text{H}_{\text{BSW}}$ of 6–9‰ during the last deglaciation.

210 3.2 Reconstruction of surface seawater isotopes based on alkenones

The $\delta^2\text{H}_{\text{C37}}$ values in core ODP 1235 ranges between -193‰ to -169‰ (Fig. 2). Between 40 ka and 25 ka the stable isotope ratio is relatively stable at ca. -180‰ then increases to -169‰ and decreases again to -173‰ at the LGM (ca. 20 ka) and down to the more negative value of -193‰ in the most recent sample. This record compares well, both in trend as well as in absolute values, with that of the previously published $\delta^2\text{H}_{\text{C37}}$ record of ODP 1234 (Weiss et al., 2019a; Fig. 2), confirming that the trends in $\delta^2\text{H}_{\text{C37}}$ happened on a regional scale. If we calculate the overall shift from the LGM (21 ka) to the most recent sample, then both records show a shift in $\delta^2\text{H}_{\text{C37}}$ of $-20 \pm 3\text{‰}$ (error indicates replicate analysis error). Published $\delta^2\text{H}_{\text{C37}}$ records from Late Quaternary sediment cores (Kasper et al., 2014; Pahnke et al., 2007; Petrick et al., 2015; Simon et al., 2015 and Weiss et al., 2019b) report $\delta^2\text{H}_{\text{C37}}$ shifts which are very similar in magnitude (see overview in Table 1) and average $-20 \pm 3\text{‰}$ for the last

deglaciation. This suggests that this shift in hydrogen isotopic composition of C₃₇ alkenones is quite similar in magnitude for
220 different oceans, despite the large differences in oceanographic settings.

Since Mix et al. (2003) observed the dominance of the open-ocean species *E. huxleyi* coccoliths in ODP 1234 and Hagino et al. (2004, 2006) and Menschel et al. (2016) showed that the dominant alkenone producer on the west coast of South America is the Group III haptophyte *E. huxleyi*, it is most likely that alkenones in both cores reflect an open-ocean Group III haptophyte signal. We can therefore apply the SPOM calibration of Gould et al. (2019) (Eq. 7) to estimate the hydrogen isotopic
225 composition of the seawater from the $\delta^2\text{H}_{\text{C}37}$. The resulting record (Fig. 2) shows a $\delta^2\text{H}_{\text{SSW}}$ value of ca. 4‰ for the uppermost sample and ca. 18‰ for the LGM for ODP 1235 (Table 1). Conversion of the shift in $\delta^2\text{H}_{\text{C}37}$ of $-20 \pm 3\text{‰}$ into $\Delta\delta^2\text{H}_{\text{SSW}}$, using the calibration of Gould et al. (2019) and considering the error in the slope of that calibration, results in a shift of $-14 \pm 4\text{‰}$ from LGM to the most recent sample. Application of the core-top calibration from Mitsunaga et al. (2022) (Eq. 8) gives an identical change of $-14 \pm 3\text{‰}$.



230

Figure 2: (a) Hydrogen isotope records of C₃₇ alkenones of ODP 1235, blue diamonds and neighbouring ODP 1234 (Weiss et al., 2019), green circles, both from the Chilean Margin. The shading represents the standard deviation of duplicate isotope measurements. Also shown are $\delta^2\text{H}$ values of surface seawater calculated using Gould et al. (2019). (b) $\delta^{18}\text{O}$ of *Uvigerina* from ODP 1235 in blue with diamonds, error bars indicate standard deviation. The green line shows the 5pt average $\delta^{18}\text{O}$ of benthic foraminifera from ODP 1234 (from de Bar et al., 2019). Published organic proxy reconstructions are shown in (c) with $\text{TEX}^{\text{H}}_{86}$ and (d) $U_{37}^{K'}$ index. SST data from ODP 1234 are from de Bar et al. (2019) and ODP 1235 from Varma et al. (2023).

3.3 Comparison of seawater isotopes and paleo salinity implications

The reconstructed $\Delta\delta^2\text{H}_{\text{ssw}}$ of ca. -14‰ from C_{37} alkenones is higher than that inferred from the benthic foraminifera isotopes (ca. -5‰) and measured in pore fluids (Schrag et al., 2002), implying that the isotopic composition of the sea surface water

240 experienced a larger change during the last deglaciation compared to the bottom water isotope composition at the Chilean Margin. Potentially, we underestimated the change in the latter due to a lack of reconstructed bottom water temperatures

However, sensitivity analysis shows that even with much smaller bottom water temperature changes than used here, the magnitude of δ^2H_{BSW} change will still be lower than that of δ^2H_{SSW} . For example, in the unlikely scenario that bottom water temperatures have remained constant, the maximum change of $\Delta\delta^{18}O_{BSW}$ is still only $-1.6 \pm 0.2\text{‰}$, or $-10.6 \pm 2\text{‰}$ of $\Delta\delta^2H_{BSW}$.

245 Thus, it seems likely that at the Chilean Margin the glacial-interglacial change in surface water isotopes was larger than that
 246 further to the north. The change in the δ^{2H}_O and δ^{13C}_C values in the interglacial is also larger than in the glacial.

of oxygen isotopes. The large regional change in $\delta^{18}\text{O}_{\text{SW}}$ could be due to changes in local climate resulting in increased precipitation and/or decreased evaporation or increased freshwater runoff, for instance. Both cores, ODP 1235 and ODP 1234, are located within the Chile–Peru upwelling system and near to two major river mouths Río Biobío and Río Itata, both draining large basins (Murati et al., 2010a). However, de Bar et al. (2018) observed no major change in the contribution of terrestrially

250 derived biomarker concentrations and in proxies for river transported material like the BIT index (Hopmans et al., 2016) and the C₃₂ 1,15-diol index (de Bar et al., 2016, Lattaud et al., 2017a, b).

To reconstruct salinity change we applied the modern open-ocean $\delta^2\text{H}_{\text{sw}}$ -salinity and $\delta^{18}\text{O}_{\text{sw}}$ -salinity relationships (Eq. 2 and 3) and a data set from 0–300 m depth. The latter set of $\delta^{18}\text{O}_{\text{sw}}$ values (n = 11) is from a surface $\delta^{18}\text{O}_{\text{sw}}$ data set

3, based on data from 0–500 meter depth). The bottom water $\Delta\text{C}_{\text{BSW}}$ based on measured salinity is ΔC values, translate using Eq. (3) and considering the error in the slope, to a change in bottom water salinity of 1 ± 0.2 psu, and are in line 255 with predictions based on a steady-state hydrodynamic model (e.g. Allison et al. 2002; Pendleton et al. 2002).

Oba et al., 2004; Waelbroeck et al., 2002). The $\Delta\delta^2\text{H}_{\text{SSW}}$ of ca. $-14\text{\textperthousand}$, based on $\delta^2\text{H}_{\text{C37}}$, translates using Eq. (2) and considering the error in the slope, to a regional salinity change of ca. 3 ± 1 psu, a larger reconstructed change than for bottom waters, but similar to the estimate of Lamy et al. (2002) who reconstructed a sea surface paleosalinity shift from 36 to 33 psu during the

last 8 ka based on $\delta^{18}\text{O}$ of planktic foraminifera for the southern Chilean Margin core ODP 1233. The observed freshening in the surface waters relative to bottom waters may be due to a stronger input in relatively low salinity waters from the Southern

Ocean (ACC/PCC) and/or more transport of low salinity Chilean Fjord Water (CFW) that, as a result of higher temperatures and intensifying continental meltwater input, resulted in even lower salinity surface water at the study site.

3.4 Global distribution of hydrogen isotope changes during last deglaciation

To examine the global distribution of hydrogen isotopes during the last deglaciation we compare the two Chilean Margin

265 records to published global alkenone hydrogen isotope records (Table 1). These comprise five low to mid-latitude records of which four show a negative glacial–interglacial shift while the record from the Mozambique Channel of Kasper et al., (2015)

reflects a positive change. The latter may be due to the close location to the river mouth, with varying freshwater input during the last 20 kyr, and therefore this record is not further considered here. If we calculate $\delta^2\text{H}_{\text{SSW}}$ from the remaining four

published $\delta^2\text{H}_{\text{C}37}$ records and compare this to our record, we find a remarkably similar negative shift from LGM to Recent in
 270 the $\delta^2\text{H}_{\text{SSW}}$ between 11–17‰ for different parts of the globe (Table 1), suggesting there might be a global aspect to this
 relatively large negative glacial–interglacial shift in surface seawater hydrogen isotope composition. This shift is larger than
 the shift inferred for bottom sea waters (e.g. Schrag et al., 2002).

There could be several reasons for this globally observed similar change in surface water hydrogen isotopic composition. For
 example, increasing average global temperatures during the deglaciation could have intensified the hydrological cycle leading
 275 to high precipitation rates and runoff (including meltwater) in many places across the globe, at least around South America
 and South Africa where most records originate from. This increased freshening of surface waters may have led to an additional
 depletion in ^2H compared to those of bottom waters. Another reason could be a change in the global waterline between the
 280 glacial and interglacial, where the slope of the $\delta^2\text{H}$ – $\delta^{18}\text{O}$ relationship changed for the surface waters. Rohling et al., (2007)
 showed, for example, that the $\delta^{18}\text{O}$ – $\delta^2\text{H}$ relationship of the evaporative Mediterranean is significantly different from that of
 the modern open-ocean and Putman et al. (2019) suggested that hydroclimate processes are important controls on the slope
 and intercept of local meteoric waterlines. Surface waters may be more sensitive to changes in the $\delta^{18}\text{O}$ – $\delta^2\text{H}$ relationship due
 to their direct atmosphere connection in contrast to bottom waters.

To verify these assumptions, further application of $\delta^2\text{H}_{\text{C}37}$ analyses of sediment cores at different open–ocean locations and
 combined $\delta^{18}\text{O}$ foraminifera analyses or pore fluid oxygen and hydrogen isotope reconstructions (Schrag et al., 2002) are
 285 needed to study the past open–ocean waterline. Extending our understanding of the (past) relationship of seawater isotopes
 and salinity could help to understand and reconstruct ocean current and ocean mixing processes.

Table 1: Comparison of the seawater isotope changes between the Last Glacial Maximum (21 ka) to Recent for different sediment cores.
 Calculated hydrogen isotopic composition of seawater is based on SPOM calibration (Gould et al., 2019) and sediment core top calibration
 290 (Mitsunaga et al., 2022). Oxygen isotopes of the bottom seawater are calculated with Cramer et al. (2011) and a temperature change estimate
 of 4 °C. For Petrick et al. (2015) a bottom water temperature change of 2 °C is estimated based on the SST data from that record.

Core	Location	Source	Recent				LGM				Difference LGM-Recent			
			Age (ka)	$\delta^2\text{H}_{\text{C}37}$ (‰)	$\delta^2\text{H}_{\text{SSW}}$ (‰)	$\delta^2\text{H}_{\text{SSW}}$ (‰) SPOM	Age (ka)	$\delta^2\text{H}_{\text{C}37}$ (‰)	$\delta^2\text{H}_{\text{SSW}}$ (‰)	$\delta^2\text{H}_{\text{SSW}}$ (‰) SPOM	$\Delta\delta^2\text{H}_{\text{C}37}$ (‰)	$\Delta\delta^2\text{H}_{\text{SSW}}$ (‰) SPOM	$\Delta\delta^2\text{H}_{\text{SSW}}$ (‰) Core top	
											Core top	Core top	Core top	
JPC32	Panama Basin	Pahnke et al. (2007)	0.3	-221	-15	-20	21.1	-198	1	-4	-23	-16	-16	
MD02-2594	Southern South Africa	Kasper et al. (2014)	3.5	-192	5	0	21.1	-173	18	13	-19	-13	-13	
l64PE304-80	Mozambique channel	Kasper et al. (2015)	0.8	-189	7	2	21.3	-196	2	-3	7	5	6	
ODP 1087	Southwest Africa	Petrick et al. (2015)	2.7	-205	-4	-9	23.1	-180	13	8	-25	-17	-17	
CD154 10-06P	Southeast Africa	Simon et al. (2015)	2	-195	3	-2	20.1	-179	14	9	-16	-11	-11	
ODP 1234	Chilean Margin	Weiss et al. (2019)	1	-195	3	-2	20.1	-176	16	11	-19	-13	-13	
ODP 1235	Chilean Margin	This study	1.1	-193	4	-1	20.6	-173	18	13	-20	-14	-14	
				Age (ka)	$\delta^{18}\text{O}_{\text{foram}}$ (‰)			Age (ka)	$\delta^{18}\text{O}_{\text{foram}}$ (‰)			$\Delta\delta^{18}\text{O}_{\text{foram}}$ (‰)	$\Delta\delta^{18}\text{O}_{\text{BSW}}$ (‰)	$\Delta\delta^2\text{H}_{\text{BSW}}$ (‰)
ODP 1234	Chilean Margin	Weiss et al. (2019)	0.78		3.3			20.1		5		-1.7	-0.9	-6.2
ODP 1235	Chilean Margin	This study	0.9		2.3			20.56		3.8		-1.5	-0.7	-4.8
ODP 1087	Southwest Africa	Petrick et al. (2015)	1.6		2.7			21.1		4		-1.3	-0.9	-6.2
LR04 stack	Global	Lisiecki and Raymo (2005)	0		3.2			20		5		-1.8	-1	-6.8

4 Conclusion

The ODP 1235 sediment record shows a large shift in $\delta^2\text{H}_{\text{C}37}$ during the last deglaciation at the Chilean Margin similar to the 295 observation reported in Weiss et al. (2019) for nearby core site ODP 1234, demonstrating that the shift is regionally consistent. The hydrogen isotope ratios of alkenones are thus a reproducible paleo proxy for relative changes in $\delta^2\text{H}_{\text{SSW}}$ and likely suggests changes in the salinity of the surface water. The reconstructed glacial–interglacial change in the hydrogen isotopic composition 300 of surface seawater is ca. $-14\text{\textperthousand}$, using either the Gould et al. (2019) or Mitsunaga et al. (2022) calibration. In contrast, the change in hydrogen isotopic composition of the bottom seawater reconstructed with the oxygen isotopic signature of benthic foraminifera was only ca. $-5\text{\textperthousand}$. Published C_{37} alkenone records from other oceans reveal a similarly large $\delta^2\text{H}_{\text{SW}}$ change. Possibly more freshening of the surface waters or a change in the slope of the modern $\delta^{18}\text{O}$ – $\delta^2\text{H}$ open–ocean waterline took place. Further application of $\delta^2\text{H}_{\text{C}37}$ analyses combined with $\delta^{18}\text{O}$ foraminifera analyses or pore fluid oxygen and hydrogen isotope reconstructions may improve our understanding of the past ocean seawater isotopic composition and salinity changes between surface and bottom water.

305 Data Availability

This study contains supplementary material. Supplement file 1 includes the age model and additional figures of the modern open–ocean salinity and isotope dataset used and cited in this study. Supplement file 2 contains the analysed isotope data of ODP 1235. The age model, sea surface temperature and isotope dataset are archived at PANGAEA (Hättig et al., 2023a,b; Varma et al., 2023).

310 Sample availability

All processed sediment samples are stored at NIOZ, i.e. TLE, Apolar, Ketone, Polar fractions of ODP 1234 and ODP 1235 core and sieved material of ODP 1235.

Author contribution

All four (co-) authors collectively contributed to the conceptualisation of this study. Devika Varma and Katrin Hättig ordered 315 samples from IODP and made sample splits for different analysis. Devika Varma prepared apolar, ketone and polar fractions and analysed alkenone and GDGTs for sea surface temperature. Katrin Hättig analysed the hydrogen isotopic composition of alkenones and performed the inorganic sample preparation, analysis, and age model computation. Visualisation of research results and original draft preparation was done by Katrin Hättig. Stefan Schouten, Marcel T. J. van der Meer and Devika Varma reviewed and edited the original draft.

The authors declare that they have no conflict of interest.

Acknowledgement

We thank Michelle Penkrot from IODP Gulf Coast Repository for providing samples of ODP site 1235. Jort Ossebaar, Ronald van Bommel and Piet van Gaever are thanked for analytical support. This work was carried out under the umbrella of the 325 Netherlands Earth System Science Centre (NESSC). This project has received funding from the European Union's Horizon 2020 research and innovation programme under the Marie Skłodowska -Curie, grant agreement No 847504.

References

Adkins, J. and Schrag, D. P.: Pore fluid constraints on deep ocean temperature and salinity during the last glacial maximum, American Geophysical Union, 28, 771–774, 2001.

330 Adkins, J. F., McIntyre, K., and Schrag, D. P.: The salinity, temperature, and $\delta^{18}\text{O}$ of the glacial deep ocean, *Science*, 298, 1769–1773, <https://doi.org/10.1126/science.1076252>, 2002.

Bakun, A.: Global Climate Change and Intensification of Coastal Ocean Upwelling, *Science*, 892, 1989

De Bar, M. W., Stolwijk, D. J., McManus, J. F., Sininghe Damsté, J. S., and Schouten, S.: A late Quaternary climate record based on long-chain diol proxies from the Chilean margin, *Clim. Past*, <https://doi.org/10.5194/cp-14-1783-2018>, 335 2018.

Bemis, B. E., Spero, H. J., Bijma, J., and Lea, D. W.: Reevaluation of the oxygen isotopic composition of planktonic foraminifera: Experimental results and revised paleotemperature equations, *Paleoceanography*, 13, 150–160, <https://doi.org/10.1029/98PA00070>, 1998.

Billups, K. and Schrag, D. P.: Paleotemperatures and ice volume of the past 27 Myr revisited with paired Mg/Ca and 340 $^{18}\text{O}/^{16}\text{O}$ measurements on benthic foraminifera, *Paleoceanography*, 17, <https://doi.org/10.1029/2000pa000567>, 2002.

Billups, K. and Schrag, D. P.: Application of benthic foraminiferal Mg/Ca ratios to questions of Cenozoic climate change, *Earth Planet. Sci. Lett.*, 209, 181–195, [https://doi.org/10.1016/S0012-821X\(03\)00067-0](https://doi.org/10.1016/S0012-821X(03)00067-0), 2003.

Blaauw, M. and Christeny, J. A.: Flexible paleoclimate age-depth models using an autoregressive gamma process, *Bayesian 345 Anal.*, 6, 457–474, <https://doi.org/10.1214/11-BA618>, 2011.

Broecker, W. S. and Comer, G.: The Glacial World according to Wally, Eldigio Press, 2002.

Brassell, S., Eglinton, G., Marlowe, I.: Molecular stratigraphy: a new tool for climatic assessment, *Nature*, 129–133, <https://doi.org/https://doi.org/10.1038/320129a0>, 1986.

Chivall, D., M'Boule, D., Sinke-Schoen, D., Sininghe Damsté, J. S., Schouten, S., van der Meer, M. T. J.: The effects

350 of growth phase and salinity on the hydrogen isotopic composition of alkenones produced by coastal haptophyte algae, *Geochim. Cosmochim. Acta*, 140, 381–390, <https://doi.org/https://doi.org/10.1016/j.gca.2014.05.043>, 2014.

Craig, H.: Isotopic Variations in Meteoric Waters, *Science*, 133, 1702–1703, <https://doi.org/10.1126/science.133.3465.1702>, 1961.

Craig, H. and Gordon, L. I.: Deuterium and oxygen 18 variations in the ocean and marine atmosphere, *Proc. Stable Isot. Oceanogr. Stud. Paleotemp. E. Tongiogi Ed.*, Spoleto, 1965.

355 Cramer, B. S., Toggweiler, J. R., Wright, J. D., Katz, M. E., and Miller, K. G.: Ocean overturning since the Late Cretaceous: Inferences from a new benthic foraminiferal isotope compilation, *Paleoceanography*, 24, <https://doi.org/10.1029/2008PA001683>, 2009.

Cramer, B. S., Miller, K. G., Barrett, P. J., and Wright, J. D.: Late Cretaceous-Neogene trends in deep ocean temperature and 360 continental ice volume: Reconciling records of benthic foraminiferal geochemistry ($\delta^{18}\text{O}$ and Mg/Ca) with sea level history, *J. Geophys. Res. Ocean.*, 116, <https://doi.org/10.1029/2011JC007255>, 2011.

Cramer, F.: Scientific colour maps (8.0.0). Zenodo. <http://doi.org/10.5281/zenodo.5501399>, 2023

Duplessy, J. C., Labeyrie, L., Juillet-Leclerc, A., Maitre, F., Duprat, J., and Sarnthein, M.: Surface salinity reconstruction of the North Atlantic Ocean during the Last Glacial maximum, *Oceanol. Acta*, 14, 311–324, 1991.

365 Duplessy, J. C., Labeyrie, L., and Waelbroeck, C.: Constraints on the ocean oxygen isotopic enrichment between the last glacial maximum and the holocene: Paleoceanographic implications, *Quat. Sci. Rev.*, 21, 315–330, [https://doi.org/10.1016/S0277-3791\(01\)00107-X](https://doi.org/10.1016/S0277-3791(01)00107-X), 2002.

Epstein, S., Buchsbaum, R., Lowenstam, H. A., and Urey, H. C.: Revised Carbonate-Water Isotopic Temperature Scale, *GSA Bull.*, 64, 1315–1326, <https://doi.org/10.1130/0016-7606,1953>, 1953.

370 Ganssen, G. M., Peeters, F. J. C., Metcalfe, B., Anand, P., Jung, S. J. A., Kroon, D., and Brummer, G. J. A.: Quantifying sea surface temperature ranges of the Arabian Sea for the past 20 000 years, *Clim. Past*, 7, 1337–1349, <https://doi.org/10.5194/cp-7-1337-2011>, 2011.

Gould, J., Kienast, M., Dowd, M., and Schefuß, E.: An open-ocean assessment of alkenone δD as a paleo-salinity proxy, *Geochim. Cosmochim. Acta*, 246, 478–497, <https://doi.org/10.1016/j.gca.2018.12.004>, 2019.

375 Hättig, K.; Varma, D.; van der Meer, M. T. J.; Reichart, G.-J.; Schouten, S. (2023a): Age model for ODP Leg 202 Site 1235 and Site 1234. PANGAEA, <https://doi.org/10.1594/PANGAEA.957070>

Hättig, K.; Varma, D.; van der Meer, M. T. J.; Schouten, S. (2023b): Hydrogen isotopic composition of alkenones and oxygen isotopes of benthic foraminifera from ODP Site 202-1235. PANGAEA, <https://doi.org/10.1594/PANGAEA.958880>

380 Häggi, C., Chiessi, C. M., and Schefuß, E.: Testing the D/H ratio of alkenones and palmitic acid as salinity proxies in the Amazon Plume, *Biogeosciences*, 12, 7239–7249, <https://doi.org/10.5194/bg-12-7239-2015>, 2015.

Hagino, K. and Okada, H.: Floral response of coccolithophores to progressive oligotrophication in the South Equatorial Current, *Pacific Ocean*, *Glob. Environ. Chang. Ocean L.*, 121–132, 2004.

385 Hagino, K. and Okada, H.: Intra- and infra-specific morphological variation in selected coccolithophore species in the equatorial and subequatorial Pacific Ocean, *Mar. Micropaleontol.*, 58, 184–206, <https://doi.org/10.1016/j.marmicro.2005.11.001>, 2006.

Hut, G.: Consultants' group meeting on stable isotope reference samples for geochemical and hydrological investigations, *Int. At. Energy Agency*, 49, 1987.

390 Kasper, S., Van Der Meer, M. T. J., Mets, A., Zahn, R., Sinnenhe Damsté, J. S., and Schouten, S.: Salinity changes in the Agulhas leakage area recorded by stable hydrogen isotopes of C37 alkenones during Termination i and II, *Clim. Past*, 10, 251–260, <https://doi.org/10.5194/cp-10-251-2014>, 2014

Lamy, F., Rühlemann, C., Hebbeln, D., and Wefer, G.: High- and low-latitude climate control on the position of the southern Peru-Chile Current during the Holocene, *Paleoceanography*, 17, 16-1–16–10, <https://doi.org/10.1029/2001pa000727>, 2002.

395 Lear, C. H., Wilson, P. A., Shackleton, N. J., and Elderfield, H.: Palaeotemperature and ocean chemistry records for the Palaeogene from Mg/Ca and Sr/Ca in benthic foraminiferal calcite, *GFF*, 122, 93, <https://doi.org/10.1080/11035890001221093>, 2000.

Lear, C. H., Rosenthal, Y., Coxall, H. K., and Wilson, P. A.: Late Eocene to early Miocene ice sheet dynamics and the global carbon cycle, *Paleoceanography*, 19, 1–11, <https://doi.org/10.1029/2004PA001039>, 2004.

400 Lear, C. H., Coxall, H. K., Foster, G. L., Lunt, D. J., Mawbey, E. M., Rosenthal, Y., Sosdian, S. M., Thomas, E., and Wilson, P. A.: Mg/Ca Paleothermometry Cross-References, *Paleoceanography*, 2004–2006, <https://doi.org/10.1002/2015PA002833>, 2015.

LeGrande, A. N. and Schmidt, G. A.: Global gridded data set of the oxygen isotopic composition in seawater, *Geophys. Res. Lett.*, 33, 1–5, <https://doi.org/10.1029/2006GL026011>, 2006.

405 Lynch-Stieglitz, J., Curry, W. B., and Slowey, N.: A geostrophic transport estimate for the Florida Current from the oxygen isotope composition of benthic foraminifera, *Paleoceanography*, 14, 360–373, <https://doi.org/10.1029/1999PA900001>, 1999.

M'boule, D., Chivall, D., Sinke-Schoen, D., Sinnenhe Damsté, J., Schouten, S., and van der Meer, M. T. J.: Salinity dependent hydrogen isotope fractionation in alkenones produced by coastal and open ocean haptophyte algae, *410 Geochim. Cosmochim. Acta*, 130, 126–135, <https://doi.org/https://doi.org/10.1016/j.gca.2014.01.029>, 2014a.

M'boule, D., Chivall, D., Sinke-Schoen, D., Sinnenhe Damsté, J. S., Schouten, S., and Van der Meer, M. T. J.: Salinity dependent hydrogen isotope fractionation in alkenones produced by coastal and open ocean haptophyte algae, *Geochim. Cosmochim. Acta*, 130, 126–135, <https://doi.org/10.1016/j.gca.2014.01.029>, 2014b.

Martin, P. A. and Lea, D. W.: A simple evaluation of cleaning procedures on fossil benthic foraminiferal Mg/Ca, *415 Geochemistry, Geophys. Geosystems*, 3, <https://doi.org/10.1029/2001GC000280>, 2002.

McCrea, J. M.: On the Isotopic Chemistry of Carbonates and a Paleotemperature Scale, *J. Chem. Phys.*, 18, 849–857, <https://doi.org/10.1063/1.1747785>, 1950.

van der Meer, M. T. J., Benthien, A., French, K. L., Epping, E., Zondervan, I., Reichart, G. J., Bijma, J., Sininghe Damsté, J. S., and Schouten, S.: Large effect of irradiance on hydrogen isotope fractionation of alkenones in *Emiliania huxleyi*, *Geochim. Cosmochim. Acta*, 160, 16–24, <https://doi.org/10.1016/j.gca.2015.03.024>, 2015.

420 Van der Meer, M. T. J., Benthien, A., Bijma, J., Schouten, S., and Sininghe Damsté, J. S.: Alkenone distribution impacts the hydrogen isotopic composition of the c37:2 and c37:3 alkan-2-ones in *emiliania huxleyi*, *Geochim. Cosmochim. Acta*, 111, 162–166, <https://doi.org/10.1016/j.gca.2012.10.041>, 2013.

425 Menschel, E., González, H. E., and Giesecke, R.: Coastal-oceanic distribution gradient of coccolithophores and their role in the carbonate flux of the upwelling system off Concepción, Chile (36°S), *J. Plankton Res.*, 38, 798–817, <https://doi.org/10.1093/plankt/fbw037>, 2016.

Mitsunaga, B. A., Novak, J., Zhao, X., Dillon, J. A., Huang, Y., and Herbert, T. D.: Alkenone $\delta^{2}\text{H}$ values – a viable seawater isotope proxy? New core-top $\delta^{2}\text{HC37:3}$ and $\delta^{2}\text{HC37:2}$ data suggest inter-alkenone and alkenone-water hydrogen isotope fractionation are independent of temperature and salinity, *Geochim. Cosmochim. Acta*, 339, 139–156, 430 <https://doi.org/10.1016/j.gca.2022.10.024>, 2022.

Mix, A., Tiedemann, R., and Blum, P.: *Proceedings of the Ocean Drilling Program, Vol. 202. Initial Reports. Southeast Pacific Paleoceanographic Transects*, *Ocean Drill. Progr.*, 2003a.

Mix, A. C., Tiedemann, R., Blum, P., and Scientists, S.: *LEG 202 SUMMARY*, *Proc. ODP, Initial Reports, 202 Coll. Station. TX (Ocean Drill. Program)*, 202, 1–145, 2003b.

435 Multizta, S., Boltovskoy, D., Donner, B., Meggers, H., Paul, A., and Wefer, G.: Temperature: $\delta^{18}\text{O}$ relationships of planktonic foraminifera collected from surface waters, *Palaeogeogr. Palaeoclimatol. Palaeoecol.*, 202, 143–152, [https://doi.org/10.1016/S0031-0182\(03\)00633-3](https://doi.org/10.1016/S0031-0182(03)00633-3), 2003.

Muratli, J. M., Chase, Z., Mix, A. C., and McManus, J.: Increased glacial-age ventilation of the Chilean margin by Antarctic Intermediate Water, *Nat. Geosci.*, 3, 23–26, <https://doi.org/10.1038/ngeo715>, 2010.

440 O’Neil, J. R., Clayton, R. N., and Mayeda, T. K.: Oxygen Isotope Fractionation in Divalent Metal Carbonates, *J. Chem. Phys.*, 51, 5547–5558, <https://doi.org/10.1063/1.1671982>, 1969.

Oba, T. and Murayama, M.: Sea-surface temperature and salinity changes in the northwest Pacific since the last glacial maximum, *J. Quat. Sci.*, 19, 335–346, <https://doi.org/10.1002/jqs.843>, 2004.

Pahnke, K., Sachs, J. P., Keigwin, L., Timmermann, A., and Xie, S. P.: Eastern tropical Pacific hydrologic changes during 445 the past 27,000 years from D/H ratios in alkenones, *Paleoceanography*, 22, 1–15, <https://doi.org/10.1029/2007PA001468>, 2007.

Pearson, P. N.: Oxygen Isotopes in Foraminifera: Overview and Historical Review, *Paleontol. Soc. Pap.*, 18, 1–38, <https://doi.org/10.1017/s1089332600002539>, 2012.

Petersen, S. V. and Schrag, D. P.: Antarctic ice growth before and after the Eocene-Oligocene transition: New estimates from clumped isotope paleothermometry, *Paleoceanography*, 30, 1305–1317, 450 <https://doi.org/10.1002/2014PA002769>, 2015.

Petrick, B. F., McClymont, E. L., Marret, F., and Van Der Meer, M. T. J.: Changing surface water conditions for the last 500ka in the Southeast Atlantic: Implications for variable influences of Agulhas leakage and Benguela upwelling, *Paleoceanography*, 30, 1153–1167, <https://doi.org/10.1002/2015PA002787>, 2015.

455 Prahl, F. G. and Wakeham, S. G.: Calibration of unsaturation patterns in long-chain ketone compositions for palaeotemperature assessment, *Nature*, 330, 367–369, <https://doi.org/10.1038/330367a0>, 1987.

Putman, A. L., Fiorella, R. P., Bowen, G. J., and Cai, Z.: A Global Perspective on Local Meteoric Water Lines: Meta-analytic Insight Into Fundamental Controls and Practical Constraints, *Water Resour. Res.*, 55, 6896–6910, <https://doi.org/10.1029/2019WR025181>, 2019.

460 Reimer, P. J., Baillie, M. G. L., Bard, E., Bayliss, A., Beck, J. W., Blackwell, P. G., Bronk Ramsey, C., Buck, C. E., Burr, G. S., Edwards, R. L., Friedrich, M., Grootes, P. M., Guilderson, T. P., Hajdas, I., Heaton, T. J., Hogg, A. G., Hughen, K. A., Kaiser, K. F., Kromer, B., McCormac, F. G., Manning, S. W., Reimer, R. W., Richards, D. A., Southon, J. R., Talamo, S., Turney, C. S. M., van der Plicht, J., and Weyhenmeyer, C. E.: IntCal09 and Marine09 Radiocarbon Age Calibration Curves, 0–50,000 Years cal BP, *Radiocarbon*, 51, 1111–1150, <https://doi.org/10.1017/S0033822200034202>, 2009.

465 Rohling, E. J.: Progress in paleosalinity: Overview and presentation of a new approach, *Paleoceanography*, 22, 1–9, <https://doi.org/10.1029/2007PA001437>, 2007.

Rohling, E. J. and Bigg, G. R.: Paleosalinity and $\delta^{18}\text{O}$: A critical assessment, *J. Geophys. Res. Ocean.*, 103, 1307–1318, <https://doi.org/10.1029/97jc01047>, 1998.

470 Rohling, E. J. and Cooke, S.: Stable oxygen and carbon isotopes in foraminiferal carbonate shells, in: *Modern Foraminifera*, Springer Netherlands, Dordrecht, 239–258, https://doi.org/10.1007/0-306-48104-9_14, 1999.

Rostek, F., Ruhlandt, G., Bassinot, F. C., Muller, P. J., Labeyrie, L. D., Lancelot, Y., and Bard, E.: Reconstructing sea surface temperature and salinity using $\delta^{18}\text{O}$ and alkenone records, *Nature*, 364, 319–321, <https://doi.org/10.1038/364319a0>, 1993.

475 Rostek, F., Bard, E., Beaufort, L., Sonzogni, C., and Ganssen, G.: Sea surface temperature and productivity records for the last 240 kyr on the Arabian Sea, *Deep. Res. Part II Top. Stud. Oceanogr.*, 44, 1461–1480, [https://doi.org/10.1016/S0967-0645\(97\)00008-8](https://doi.org/10.1016/S0967-0645(97)00008-8), 1997.

Sachs, J. P. and Kawka, O. E.: The influence of growth rate on $2\text{H}/1\text{H}$ fractionation in continuous cultures of the coccolithophorid *Emiliania huxleyi* and the diatom *Thalassiosira pseudonana*, *PLoS One*, 10, <https://doi.org/10.1371/journal.pone.0141643>, 2015.

480 Sachs, J. P., Maloney, A. E., Gregersen, J., and Paschall, C.: Effect of salinity on $2\text{H}/1\text{H}$ fractionation in lipids from continuous cultures of the coccolithophorid *Emiliania huxleyi*, *Geochim. Cosmochim. Acta*, 189, 96–109, <https://doi.org/https://doi.org/10.1016/j.gca.2016.05.041>, 2016.

Schouten, S., Hopmans, E. C., Schefuß, E., and Sinninghe Damsté, J. S.: Corrigendum to “Distributional variations in marine 485 crenarchaeotal membrane lipids: a new tool for reconstructing ancient sea water temperatures?,” *Earth Planet. Sci.*

Lett., 211, 205–206, [https://doi.org/10.1016/s0012-821x\(03\)00193-6](https://doi.org/10.1016/s0012-821x(03)00193-6), 2003.

Schouten, S., Ossebaar, J., Schreiber, K., Kienhuis, M. V. M., Langer, G., Benthien, A., and Bijma, J.: The effect of temperature, salinity and growth rate on the stable hydrogen isotopic composition of long chain alkenones produced by *Emiliania huxleyi* and *Gephyrocapsa oceanica*, *Biogeosciences*, 3, 113–119, <https://doi.org/10.5194/bg-3-113-2006>, 2006.

Schrag, D. P., Adkins, J. F., McIntyre, K., Alexander, J. L., Hodell, D. A., Charles, C. D., and McManus, J. F.: The oxygen isotopic composition of seawater during the Last Glacial Maximum, *Quat. Sci. Rev.*, 21, 331–342, [https://doi.org/https://doi.org/10.1016/S0277-3791\(01\)00110-X](https://doi.org/https://doi.org/10.1016/S0277-3791(01)00110-X), 2002.

Shackleton, N. J.: Attainment of isotopic equilibrium between ocean water and the benthonic foraminifera genus *Uvigerina*: Isotopic changes in the ocean during the last glacial, *Colloq. Int. du C.N.R.S.*, 219, 203–210, 1974.

Simon, M. H., Gong, X., Hall, I. R., Ziegler, M., Barker, S., Knorr, G., Van Der Meer, M. T. J., Kasper, S., and Schouten, S.: Salt exchange in the Indian-Atlantic Ocean Gateway since the Last Glacial Maximum: A compensating effect between Agulhas Current changes and salinity variations?, *Paleoceanography*, 30, 1318–1327, <https://doi.org/10.1002/2015PA002842>, 2015.

Spero, H. J., Bijma, J., Lea, D. W., and Bemis, B. E.: Effect of seawater carbonate concentration on foraminiferal carbon and oxygen isotopes, *Lett. to Nat.*, 390, 497–500, 1997.

Spero, H. J., Mielke, K. M., Kalve, E. M., Lea, D. W., and Pak, D. K.: Multispecies approach to reconstructing eastern equatorial Pacific thermocline hydrography during the past 360 kyr, *Paleoceanography*, 18, <https://doi.org/10.1029/2002PA000814>, 2003.

Srivastava, R., Ramesh, R., Jani, R. A., Anilkumar, N., and Sudhakar, M.: Stable oxygen, hydrogen isotope ratios and salinity variations of the surface Southern Indian Ocean waters, *Curr. Sci.*, 99, 1395–1399, 2010.

Strub, P. T., Mesías, M. J., Montecino, V., Rutllant, J., and Salinas, S.: Coastal ocean circulation off western South America coastal segment, 1998.

Tang, C. M. and Stott, L. D.: provide insight into the dynamics of monsoon In this study , we analyzed the stable isotopic composition of individual planktonic foraminifera after sapropel formation . Because individual single foraminiferal tests to the investigation of salinity change, 8, 473–493, 1993.

Varma, D.; Hättig, K.; van der Meer, M. T. J.; Reichart, G.-J.; Schouten, S. (2023a): SST Proxies Chilean (ODP Leg 202 Site 1235 and Site 1234) and Angola Margin (ODP Leg 175 Site 1078 and Site 1079). PANGAEA, <https://doi.org/10.1594/PANGAEA.957090>

Varma, D., Hättig, K., van der Meer, M. T. J., Reichart, G. J., and Schouten, S.: Constraining Water Depth Influence on Organic Paleotemperature Proxies Using Sedimentary Archives, *Paleoceanogr. Paleoclimatology*, 38, <https://doi.org/10.1029/2022PA004533>, 2023.

Waelbroeck, C., Labeyrie, L., Michel, E., Duplessy, J. C., McManus, J. F., Lambeck, K., Balbon, E., and Labracherie, M.: Sea-level and deep water temperature changes derived from benthic foraminifera isotopic records, *Quat. Sci. Rev.*,

Weiss, G. M., Schouten, S., Sinninghe Damsté, J. S., and van der Meer, M. T. J.: Constraining the application of hydrogen isotopic composition of alkenones as a salinity proxy using marine surface sediments, *Geochim. Cosmochim. Acta*, 250, 34–48, <https://doi.org/10.1016/j.gca.2019.01.038>, 2019a.

Weiss, G. M., Schouten, S., Sinninghe Damsté, J. S., and van der Meer, M. T. J.: Constraining the application of hydrogen isotopic composition of alkenones as a salinity proxy using marine surface sediments, *Geochim. Cosmochim. Acta*, 250, 34–48, <https://doi.org/10.1016/j.gca.2019.01.038>, 2019b.

Weiss, G. M., de Bar, M. W., Stolwijk, D. J., Schouten, S., Sinninghe Damsté, J. S., and van der Meer, M. T. J.: Paleosensitivity of Hydrogen Isotope Ratios of Long-Chain Alkenones to Salinity Changes at the Chile Margin, *Paleoceanogr. Paleoclimatology*, 34, 978–989, <https://doi.org/10.1029/2019PA003591>, 2019c.

Weiss, G. M., Pfannerstill, Y. E., Schouten, S., Sinninghe Damsté, S. J., and van der Meer, T. J. M.: Effects of alkalinity and salinity at low and high light intensity on hydrogen isotope fractionation of long-chain alkenones produced by *Emiliania huxleyi*, *Biogeosciences*, 14, 5693–5704, <https://doi.org/10.5194/bg-14-5693-2017>, 2017.

Zhang, X., Gillespie, A. L., and Sessions, A. L.: Large D/H variations in bacterial lipids reflect central metabolic pathways, *Proc. Natl. Acad. Sci. U. S. A.*, 106, 12580–12586, <https://doi.org/10.1073/pnas.0903030106>, 2009.

Zhang, Z. and Sachs, J. P.: Hydrogen isotope fractionation in freshwater algae: I. Variations among lipids and species, *Org. Geochem.*, 38, 582–608, [https://doi.org/https://doi.org/10.1016/j.orggeochem.2006.12.004](https://doi.org/10.1016/j.orggeochem.2006.12.004), 2007.

Zweng, M. M., J. R. Reagan, D. Seidov, T. P. Boyer, R. A. Locarnini, H. E. Garcia, A. V. Mishonov, O. K. Baranova, K. Weathers, C. R. P. and Smolyar, I.: World Ocean Atlas 2018, 2:Salinity, 82, 50, 2018